Proc. Natl. Acad. Sci. USA
Vol. 81, pp. 38–42, January 1984
Biochemistry

Rearrangement of a DNA sequence homologous to a cell–virus junction fragment in several Moloney murine leukemia virus-induced rat thymomas

(T-cell lymphoma/provirus/specific integration site)

GUY LEMAY* AND PAUL JOLICOEUR*†

*Institut de Recherches Cliniques de Montréal, 110 Avenue des Pins ouest, Montréal, Québec, Canada; and †Département de Microbiologie et d'Immunologie, Université de Montréal, Montréal, Québec, Canada

Communicated by Henry S. Kaplan, September 6, 1983

ABSTRACT **We have studied the integrated proviruses in Moloney murine leukemia virus-induced rat thymomas. By Southern blot analysis, we found several complete integrated proviruses in each tumor. In most tumors, we could not detect defective or recombinant proviruses. Several of these integrated proviruses (with their flanking cellular sequences) from a single tumor were cloned in Charon 4A. Their flanking cellular fragments were subcloned into pBR322 and used as a probe to screen other thymoma DNAs. With one clone (pMo-1C) used as a probe, we could detect novel fragments in 11 out of 20 thymoma DNAs analyzed. In three of these thymomas we could analyze in more detail, it appears that these novel fragments are generated by the insertion of a provirus. This specific integration of Moloney provirus in the host genome may represent an important genetic event leading to tumor formation.**

The nondefective retroviruses generally induce malignant diseases after a long latency period. The mechanism by which they transform cells is beginning to emerge. They do not seem to harbor an oncogene, but the 3′ end of their genome (1), more specifically the U3 long terminal repeat (LTR) (2, 3), appears to be required for tumor induction. Avian leukosis virus- and reticuloendotheliosis virus-induced tumors have been shown to contain proviruses integrated in the proximity of the *myc* oncogene (4–8) and activating its transcription (5, 6). Recently, it has been shown that several mouse mammary tumor virus-induced tumors contain a provirus integrated in a specific domain of the host genome (9), a finding also compatible with the activation of a specific oncogene by this provirus. To determine whether the Moloney murine leukemia virus (Mo-MuLV) induces disease by a similar mechanism, we first studied the specificity of Moloney proviruses integration into the host genome. We took advantage of the apparent clonality of the tumors (thymoma) induced by this virus for our studies. By cloning several proviruses with their flanking cellular sequences from one rat thymoma, we identified one cellular sequence that appeared rearranged in several other thymomas.

MATERIALS AND METHODS

Animals. Pregnant female Fisher 344 and Lewis inbred rats were obtained from Charles River Breeding Laboratories. Newborn (<48-hr-old) rats were inoculated intraperitoneally or intrathymically with 10^5 plaque-forming units of Mo-MuLV (clone 1) (10).

DNA Extraction and Endonuclease Digestion. DNA was extracted from primary thymomas or from normal rat liver and digested with various restriction endonucleases (New England BioLabs and Boehringer Mannheim) as described (11).

Agarose Slab Gel Electrophoresis and Hybridization Procedure. DNA analysis by agarose gel electrophoresis and transfer to a nitrocellulose membrane were done by the technique of Southern (12), as described (11). The ^{32}P-labeled probes used for hybridization are described in *Results*. They were labeled by nick-translation as described (13).

Molecular Cloning Procedures. Tumor F10 DNA was digested with *Eco*RI and fragments (1 μg) of 10–20 kilobase pairs (kbp) enriched on a sucrose density gradient (11) were ligated to purified *Eco*RI arms of Charon 4A (2 μg) as described (14, 15). This ligated DNA was packaged and 10^6 phages were screened with a Mo-MuLV representative cloned DNA (16) probe, as described (11, 14, 15). Subcloning into pBR322 was done as before (11).

RESULTS

Structure of Mo-MuLV Proviruses in Rat Tumor Cells. A high percentage of inbred Fisher 344 (70%) and Lewis (80%) newborn rats inoculated with Mo-MuLV (clone 1) (10) had a thymoma after a latency period of 3–6 months. About 30% of rats with a thymoma also had an enlarged spleen.

To analyze the integrated Moloney proviruses in these rat thymoma DNAs, we first used a restriction endonuclease analysis by the Southern blot procedure. *Eco*RI was most suitable for this analysis because it does not cleave the Mo-MuLV genome (16, 17), and therefore allows the detection of each newly acquired Moloney provirus flanked by its right and left cellular junction fragments. Several virus-specific fragments could be detected with a representative Mo-MuLV probe in all the 30 thymoma DNAs tested (Fig. 1*A* and unpublished data). Not a single tumor tested harbored fewer than five newly integrated proviruses.

The same analysis performed on the same DNAs with a LTR-specific probe revealed no virus-specific fragment in normal rat DNA and essentially the same pattern of integrated proviruses as the one detected with the representative probe in tumor DNAs (Fig. 1*B* and unpublished data). Only 2 tumor DNAs (L3 and L4) were found to harbor an additional fragment hybridizing with the LTR probe but not with the representative probe [Fig. 1 (lane i) and unpublished data]. These fragments, which are likely to represent highly defective proviruses, were not studied further. Twenty tumor DNAs were digested with restriction endonucleases that cleave Mo-MuLV DNA internally. Cleavage of most tumor DNAs with *Xba* I showed the expected internal 2.4- and 5.6-kbp Mo-MuLV fragments (Fig. 1*C*). Only 2 tumor DNAs out of 20 (F10, F16) were found to harbor additional *Xba* I fragments [Fig. 1 (lane n) and unpublished data]. The provirus giving rise to these aberrant *Xba* I fragments in F10 was

The publication costs of this article were defrayed in part by page charge payment. This article must therefore be hereby marked "*advertisement*" in accordance with 18 U.S.C. §1734 solely to indicate this fact.

Abbreviations: Mo-MuLV, Moloney murine leukemia virus; LTR, long terminal repeat; kbp, kilobase pair(s).

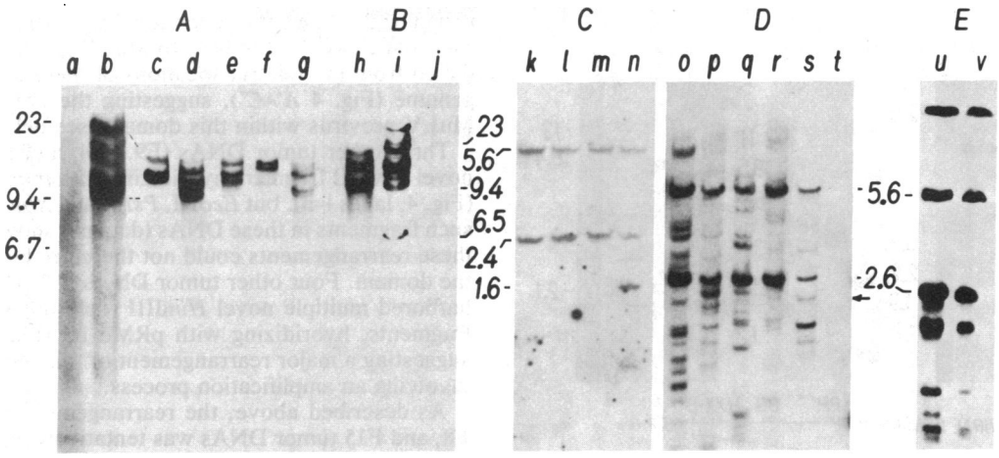

FIG. 1. Analysis of integrated proviruses in Mo-MuLV-induced rat thymomas. DNAs from representative primary thymoma or from normal Fisher 344 rat liver were extracted and digested with restriction endonucleases. The DNA fragments (20 μg) were separated by 1% agarose gel electrophoresis, transferred to nitrocellulose filters, and hybridized with the ^{32}P-labeled representative Mo-MuLV cloned DNA probe (*A* and *C*) or the LTR (18) probe (*B*, *D*, and *E*). (*A* and *B*) Normal rat liver DNA (lanes a and j) or DNA from thymomas F10 (lanes b and h), L2 (lane c), L4 (lanes d and i), L3 (lane e), L7 (lane f), and F8 (lane g) were digested with *Eco*RI. (*C*) Thymoma L7, F8, F9, and F10 DNAs (lanes k–n) were digested with *Xba* I. (*D*) Thymoma L4, L5, L6, L7, and F10 DNAs (lanes o–s) and normal liver DNA (lane t) were digested with *Sac* I. (*E*) DNAs extracted from the thymoma (lane u) and the infiltrated spleen (lane v) of the same leukemic rat (F15) were digested with *Sac* I. Arrow, left virus–cell junction fragment, subsequently cloned in Charon 4A. Numbers, kbp.

cloned in Charon 4A and shown to have a point mutation at nucleotide 6,564 (19), thus generating a new *Xba* I site in the *env* region (data not shown). A similar analysis using the representative probe was also carried out with *Sac* I and *Pvu* II. The expected internal *Sac* I (2.6- and 5.6-kbp) and *Pvu* II (3.3-, 1.6-, and 0.9-kbp) fragments but no other aberrant virus-specific fragments were found in all the 20 tumor DNAs analyzed (data not shown). These results show that most of the numerous proviruses found in Mo-MuLV-induced rat thymomas do not appear to have a recombinant genome.

The same 20 tumor DNAs were digested with *Sac* I and hybridized with the LTR probe to study the right and left virus–cell junction fragments. Several such fragments were detected in addition to the 2.6- and 5.6-kbp internal *Sac* I fragments (Fig. 1*D* and unpublished data). They form a unique band pattern for each tumor. In the four animals studied, this pattern was identical in the primary thymoma and in the infiltrated spleen DNA from the same rat (Fig. 1*E* and unpublished data), suggesting that these thymomas are clonal.

Molecular Cloning of Several Moloney Provirus Integration Sites of One Thymoma. To test the specificity of Mo-MuLV provirus integration, we cloned several integrated proviruses of a single tumor (F10) that appears to harbor a lower number of newly integrated proviruses (Fig. 1, lanes b and h). We ligated Charon 4A *Eco*RI arms with *Eco*RI-digested F10 DNA to obtain recombinant phages, which were screened with the representative Mo-MuLV probe. Eleven recombinants, which fell into 4 classes, were isolated, purified, and subcloned into pBR322 at the *Eco*RI site. A cellular fragment from one clone of each class was then subcloned into pBR322, mapped, and used as a probe to screen other tumor DNAs. Clone pRMo-1 was found to harbor a cellular sequence that appeared rearranged in several tumors (see below). pRMo-1 DNA was infectious in a transfection assay on NIH/3T3 cells (data not shown). Its restriction map is shown in Fig. 2. The restriction map of this Moloney provirus was identical to that of the Mo-MuLV genome (17) at the 38 sites tested (Fig. 2 and unpublished data). The *Eco*RI/*Sal* I cellular fragment subcloned into pBR322 (Fig. 2) was designated pRMo-1C and used as a probe for subsequent work.

Physical Mapping of RMoInt-1, the Normal Rat Cellular Sequence Homologous to pRMo-1C. To detect and map possible rearrangements around the sequence recognized by pRMo-1C, we mapped this region in normal rat DNA. The pRMo-1C probe detected single *Eco*RI (2.2-kbp), *Pst* I (8.5-kbp), *Xba* I (8.4-kbp), and *Bam*HI (20-kbp) fragments in normal rat DNA and, as expected, two *Hin*dIII fragments (3.3 and 1.3 kbp) (Fig. 3*A*). Double digestion with *Hin*dIII/*Pst* I and *Hin*dIII/*Eco*RI were used to map these sites relative to each other (Fig. 3, lanes c and d). The *Eco*RI (2.2-kbp) and the *Hin*dIII/*Eco*RI (1.7- and 0.5-kbp) fragments detected in normal DNA had the same length as the sum of the right and left cellular sequences on clone pRMo-1, suggesting that no major deletion or duplication of the adjacent cellular sequences had occurred around this integration site. This was confirmed by the detection of the same 2.2-kbp *Eco*RI, 3.3-kbp *Hin*dIII, 1.9-kbp *Hin*dIII/*Pst* I and 1.7-kbp *Hin*dIII/*Eco*RI fragments (Fig. 3*B*), with both probe RMo-1r (prepared from the right cellular flanking sequence) (Fig. 2) and the pRMo-1C probe. Digestion of F10 DNA from which pRMo-1 was cloned was also used to map the integration site. By comparing the length of the normal sequence with that of the rearranged sequence using restriction enzymes whose sites were mapped on the pRMo-1 clone, we derived a partial restriction map of this cellular domain spanning about 20 kbp.

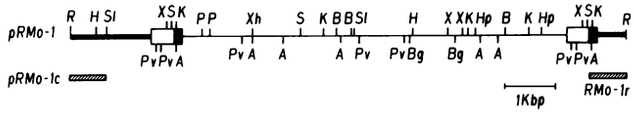

FIG. 2. Restriction endonuclease mapping of the pRMo-1 DNA clone. λRMo-1 recombinant phage was cleaved with *Eco*RI and the 11.0-kbp insert was subcloned in pBR322 at the *Eco*RI site. This clone was designated pRMo-1. For mapping, plasmid pRMo-1 DNA was digested first with *Eco*RI and then with other restriction endonucleases. DNA fragments were electrophoresed on a 1.4% agarose gel and visualized with ethidium bromide. They were transferred to a nitrocellulose membrane and hybridized with the ^{32}P-labeled representative Moloney probe. Fragments size was estimated by using *Hin*dIII-digested λ DNA fragments as markers. The left 0.7-kbp *Eco*RI/*Sal* I cellular fragment was subcloned into pBR322 and this clone was designated pRMo-1C. The right 0.7-kbp *Sac* I/*Eco*RI fragment (designated pMo-1r) was electroeluted and used as a probe. Open box, U3 LTR; black box, U5 LTR; thin line, complete Moloney provirus; thick line, cellular sequences. Restriction sites: A, *Ava* I; B, *Bam*HI; Bg, *Bgl* I; H, *Hin*dIII; Hp, *Hpa* I; K, *Kpn* I; P, *Pst* I; Pv, *Pvu* II; R, *Eco*RI; S, *Sac* I; Sl, *Sal* I; X, *Xba* I; Xh, *Xho* I.

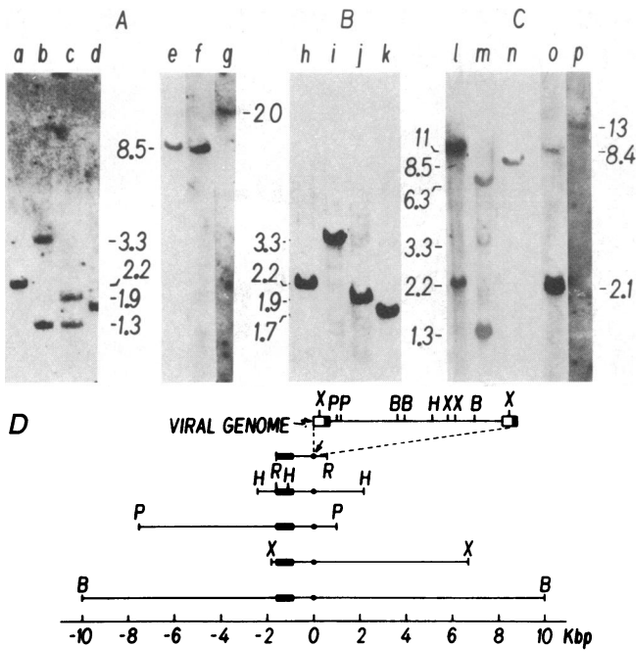

FIG. 3. Partial restriction map of the normal rat cellular sequence homologous to pRMo-1. Normal rat DNA or DNA from thymoma F10 from which the pRMo-1 clone was derived was digested with restriction endonucleases and DNA samples (20 μg) were separated on a 1% agarose gel, transferred to nitrocellulose filters, and hybridized with the ^{32}P-labeled 0.7-kbp *Eco*RI/*Sal* I cloned fragment (pRMo-1C) or the ^{32}P-labeled 0.7-kbp *Eco*RI/*Sac* I-purified right cellular fragment (RMo-1r). (*A* and *B*) Fisher 344 rat liver DNA was digested with *Eco*RI (lanes a and h), *Hin*dIII (lanes b and i). *Hin*dIII/*Pst* I (lanes c and j), *Hin*dIII/*Eco*RI (lanes d and k), *Pst* I (lane e), *Xba* I (lane f), or *Bam*HI (lane g) and hybridized with the pRMo-1C (*A*) or the RMo-1r (*B*) probe. (*C*) F10 DNA was digested with *Eco*RI, *Hin*dIII, *Pst* I, *Xba* I, or *Bam*HI (lanes l–p) and hybridized with the pRMo-1C probe. (*D*) Partial restriction map of the normal sequences flanking the RMo-1 sequence. The site of integration of the 8.8-kbp Moloney provirus within this domain in F10 is shown by an arrow and a point. Open and black boxes, LTR; hatched boxes, normal sequence homologous to pRMo-1C cloned DNA. Symbols are as in Fig. 2. Numbers, kbp.

For example, using *Xba* I, *Pst* I, *Bam*HI, and *Hin*dIII, which cleave at 0.3, 1.0, 3.6, and 5.2 kbp within the Moloney provirus (ref. 16; Fig. 2), we mapped these sites at 1.8, 7.5, 9.4, and 1.1 kbp, respectively, from the left LTR simply by measuring the lengths of the rearranged fragments (respectively, 2.1, 8.5, 13, and 6.3 kbp) (Fig. 3*C*). With these sites mapped at the left, we then mapped the sites for the same enzymes at the right of the provirus by simply measuring the length of the fragment generated by each restriction endonuclease in normal DNA, assuming these sequences are identical in normal and F10 DNA. We have shown above that this assumption is valid. The partial map thus generated (Fig. 3) is identical for Fisher 344 and Lewis rat DNA.

Rearrangements of RMoInt-1 Sequences in 11 Different Mo-MuLV-Induced Rat Thymomas. We used probe pRMo-1C to determine whether this domain has been rearranged in other rat thymoma DNAs. We detected a novel DNA fragment in 11 out of 20 tumor DNAs analyzed, in addition to the normal fragment always present (Fig. 4). Using the restriction map we had previously derived, we partially mapped the rearrangement within this domain for three additional tumors. L3 showed nearly the same rearrangement as F10, from which pRMo-1C was cloned (Fig. 4*A*). F8 and F15 each harbor a rearranged sequence, which was tentatively mapped at the left of the sequence recognized by pRMo-1C (Fig. 4 *B* and *C*). In each of these 3 tumor DNAs, the lengths of the rearranged fragments generated by restriction endonucleases that cleave within the Mo-MuLV genome could be predicted from the relative locations of these sites on the viral genome (Fig. 4 *A'*–*C'*), suggesting the presence of a Mo-MuLV provirus within this domain (see below).

Three other tumor DNAs (F9, F14, and F16) harbored a novel *Hin*dIII fragment hybridizing with the pRMo-1C probe (Fig. 4, lanes l–n), but *Eco*RI, *Pst* I, and *Xba* I did not reveal such fragments in these DNAs (data not shown). The sites of these rearrangements could not therefore be mapped within the domain. Four other tumor DNAs (L2, L3, L7, and F11) harbored multiple novel *Hin*dIII (data not shown) or *Pst* I fragments, hybridizing with pRMo-1C (Fig. 4, lanes o–r), suggesting a major rearrangement of this region, most likely involving an amplification process.

As described above, the rearrangement observed in L3, F8, and F15 tumor DNAs was tentatively mapped assuming the presence of a provirus close to the sequence recognized by pRMo-1C. To validate this assumption further, two of these tumor DNAs were studied in more detail. If, indeed, the rearrangement observed in these tumors was the consequence of the presence of an integrated Mo-MuLV provirus in the orientation we expected, the putative right cell–virus junction fragment should hybridize with both a virus-specific and the pRMo-1C probe. Tumor F8 DNA was therefore digested with *Pst* I/*Bam*HI or *Pst* I/*Hin*dIII and first hybridized with the pRMo-1C probe. Single rearranged fragments of, respectively, 4.9 and 4.6 kbp were observed (Fig. 5 *A* and *B*, lane a). The same filter was washed, reexposed, to monitor the absence of signals, and hybridized with *env* probe. Several bands could be detected, as expected. One of these *env*-specific fragments comigrated exactly with the 4.9- and 4.6-kbp fragments previously detected with the pRMo-1C probe (Fig. 5 *A* and *B*, lanes b), suggesting the presence of proviral DNA on this fragment. Similar results were obtained with F15 DNA (Fig. 5*C*).

DISCUSSION

To avoid the high background of endogenous proviruses present in the mouse genome, we have chosen the rat as the host for the induction of thymoma by Mo-MuLV. In each of the 30 thymomas analyzed, we found a relatively high number of integrated proviruses. This is in contrast with the low copy number and the numerous defective proviruses detected in avian leukosis-induced tumors (4, 7, 20). In the majority of the tumors, we could not detect defective or recombinant proviruses, in contrast with the recombinant (MCF-type) proviruses detected in most mouse Mo-MuLV-induced thymomas (21). This finding suggests that the presence of these recombinant proviruses is not essential for tumor formation, at least in rat.

Using, as a probe, a cellular sequence flanking a provirus from one of these thymomas, we identified a rearrangement of this domain in a significant percentage of the thymomas. A detailed analysis of these fragments in a few thymomas is consistent with the fact that they are generated by the insertion of a provirus. They are unlikely to have arisen through restriction endonuclease polymorphism because inbred rats were used for these studies and because an analysis with three other different probes, derived from cell–virus junction fragments and hybridizing with unique-copy DNA, did not reveal any polymorphism in the 20 thymoma DNAs.

Such an integration of a provirus into a specific domain has been described previously in avian leukosis (4–7), reticuloendotheliosis (8) and mouse mammary (9) virus-induced tumors. In avian leukosis- and reticuloendotheliosis-virus-induced tumors, the provirus was shown to be integrated close to the *myc* oncogene, suggesting that this event is involved in tumorigenesis. While we were writing this manuscript, Tsichlis *et al.* (22) reported the integration of a provi-

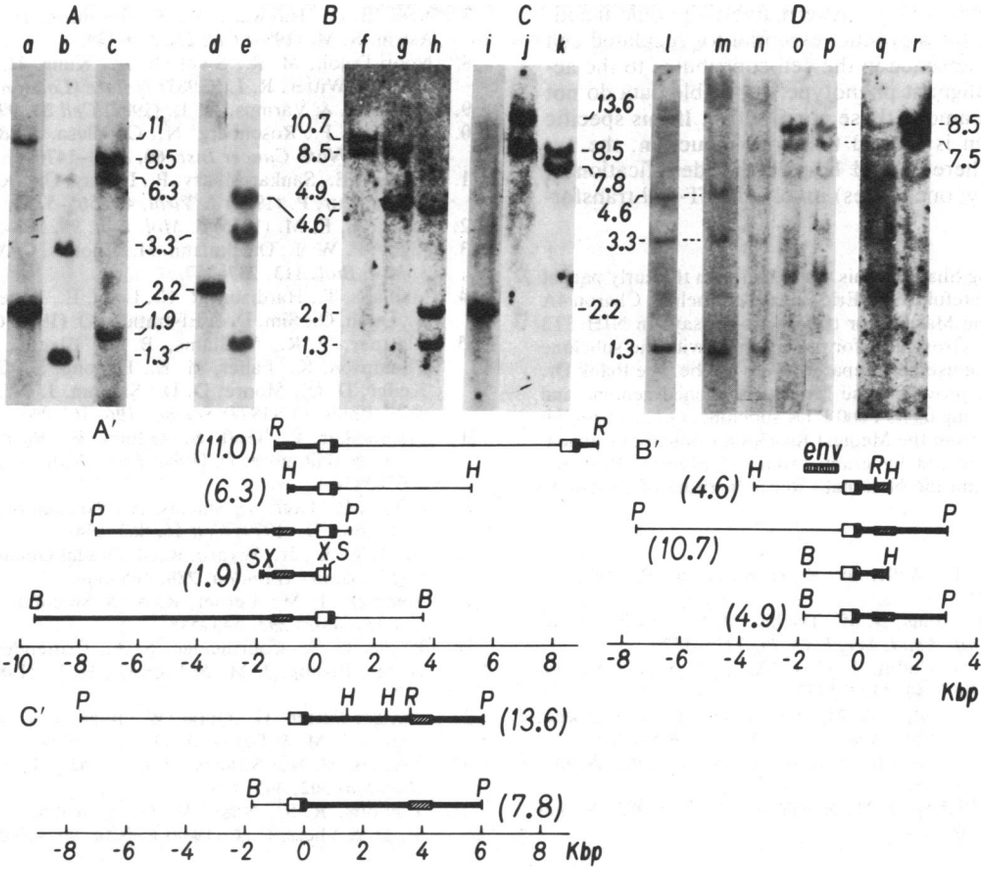

FIG. 4. Novel DNA fragments homologous to pRMo-1 detected in 10 additional thymoma DNAs. DNAs (20 μg) from thymomas were digested with various restriction endonucleases and electrophoresed onto 1% agarose gels, transferred to nitrocellulose filters, and hybridized with ^{32}P-labeled pRMo-1C DNA. (*A*) Thymoma L3 DNA was digested with *Eco*RI, *Hin*dIII, and *Xba* I (lanes a–c). (*B*) Thymoma F8 DNA was digested with *Eco*RI, *Hin*dIII, *Pst* I, *Pst* I/*Bam*HI, and *Pst* I/*Hin*dIII (lanes d–h). (*C*) Thymoma F15 DNA was digested with *Eco*RI, *Pst* I, and *Pst* I/*Bam*HI (lanes i–k). (*D*) DNA from thymomas F9, F14, and F16 (lanes l–n) was digested with *Hin*dIII and DNA from thymomas L2, L3, L7, and F11 (lanes o–r) was digested with *Pst* I. (*A'–C'*) Corresponding partial restriction maps of the novel DNA fragments, with their lengths (kbp) in parentheses. *env*, Envelope. Symbols are as in Fig. 2.

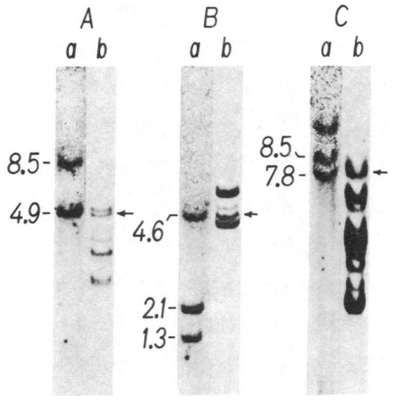

FIG. 5. Novel DNA fragments hybridizing with pRMo-1C and *env* probes in thymomas F15 and F8. DNA (20 μg) from F8 (*A* and *B*) and F15 (*C*) was digested with *Pst* I/*Bam*HI (*A* and *C*) or *Pst* I/*Hin*dIII (*B*) and electrophoresed on a 1% agarose gel. DNA fragments were transferred to nitrocellulose filters and hybridized with the ^{32}P-labeled pRMo-1C probe (lanes a). The filters were then washed at 80°C for 1 hr with 7.5 mM NaCl/0.75 mM Na citrate, reexposed to monitor the efficiency of the washing procedure, and hybridized with the ^{32}P-labeled *env* probe (lanes b). The *env* fragment was prepared by digesting a subclone of Mo-MuLV DNA (16) with *Bam*HI and *Cla* I and purifying the 1.1-kbp fragment by agarose gel electrophoresis followed by electroelution. Its location on the viral genome is shown in Fig. 4. Arrows indicate the fragment hybridizing with both probes.

rus in a common domain of Mo-MuLV-induced Osborn Mendel rat thymomas. It is not clear at this point whether the RMoInt-1 sequence we identified is the same as the one characterized by those workers, but the restriction maps of these two sequences differ significantly.

The significance of our findings in the context of oncogenesis is unclear. This specific rearrangement may be unrelated to oncogenesis and the RMoInt-1 region may simply represent a preferred integration site for Moloney proviruses, as it appears for the human *BEVI* locus and the baboon provirus (23). This seems unlikely and, in fact, this region does not appear to be a preferential site of integration considering that only 11 out of the 100–200 proviruses detected in the 20 thymomas analyzed were integrated in this domain and, in each case, in only one chromosome. Alternatively, this specific rearrangement may represent one important genetic event leading to tumor formation. A provirus could integrate in this region (preferentially or at random) and the cell harboring such a rearranged domain (and possibly other changes) could become transformed, gain a growth advantage, and form a tumor. The apparent clonality of the thymomas would be compatible with this selection hypothesis. The high number of integrated proviruses suggests the need for more than one event for tumor induction.

The mechanism by which such an integrated provirus in RMoInt-1 domain could lead to T-cell transformation remains obscure. The provirus could activate the transcription of an adjacent gene whose product is essential for transformation, as proposed for the c-*myc* activation by the avian

leukemia virus provirus (5, 6). Alternatively, it could inactivate a gene coding for a product essential for regulated cell growth and whose absence in the cell contributes to the acquisition of the malignant phenotype. Available data do not allow us to choose among these possibilities. If this specific provirus integration is critical to tumor induction, the approach described here should help in the identification of genes (possibly new oncogenes) involved in T-cell transformation.

We thank Dr. Ming Shang for his contribution in the early part of this work. We are grateful to Dr. Eric Rassart for help in Charon 4A preparation, to Sylvie Masson for transfection assays in NIH/3T3 cells, and to Luc DesGroseillers for providing us with the subclone of Mo-MuLV genome used to prepare the *env* probe. We thank Dr. David Baltimore for providing the Mo-MuLV cloned genome and Dr. Dino Dina for giving us its P600 LTR subclone. G.L. is a recipient of a studentship from the Medical Research Council of Canada. This work was supported by grants from the Medical Research Council of Canada and the National Cancer Institute of Canada to P.J.

1. DesGroseillers, L., Villemur, R. & Jolicoeur, P. (1983) *J. Virol.* **47,** 24–32.
2. Robinson, H. L., Blais, B. M., Tsichlis, P. N. & Coffin, J. M. (1982) *Proc. Natl. Acad. Sci. USA* **79,** 1225–1229.
3. Tsichlis, P. N. & Coffin, J. M. (1979) *Cold Spring Harbor Symp. Quant. Biol.* **44,** 1123–1132.
4. Fung, Y. K. T., Fadly, A. M., Crittenden, L. B. & Kung, H. J. (1981) *Proc. Natl. Acad. Sci. USA* **78,** 3418–3422.
5. Hayward, W. S., Neel, B. G. & Astrin, S. M. (1981) *Nature (London)* **290,** 475–480.
6. Payne, G. S., Bishop, J. M. & Varmus, H. E. (1982) *Nature (London)* **295,** 209–214.
7. Neel, B. G., Hayward, W. S., Robinson, H. L., Fang, J. & Astrin, S. M. (1981) *Cell* **23,** 323–334.
8. Noori-Daloii, M. R., Swift, R. A., Kung, H. J., Crittenden, L. M. & Witter, R. L. (1981) *Nature (London)* **294,** 574–576.
9. Nusse, R. & Varmus, H. E. (1982) *Cell* **31,** 99–109.
10. Jolicoeur, P., Rosenberg, N., Cotellesa, A. & Baltimore, D. (1978) *J. Natl. Cancer Inst.* **60,** 1473–1476.
11. Rassart, E., Sankar-Mistry, P., Lemay, G., DesGroseillers, L. & Jolicoeur, P. (1983) *J. Virol.* **45,** 565–575.
12. Southern, E. M. (1975) *J. Mol. Biol.* **98,** 503–517.
13. Rigby, P. W. J., Dieckmann, M., Rhodes, C. & Berg, P. (1977) *J. Mol. Biol.* **113,** 237–257.
14. Maniatis, T., Hardison, R. C., Lacy, E., Laver, J., O'Connel, C., Quon, C., Sim, D. & Efstratidis, O. (1978) *Cell* **15,** 687–701.
15. Blattner, F. R., Williams, B. G., Blechl, A., Denniston-Thompson, K., Faber, M. E., Furlong, L., Grunwald, D. J., Keifer, D. O., Moore, D. D., Shumm, J. W., Sheldon, E. L. & Smithies, O. (1977) *Science* **196,** 161–169.
16. Shoemaker, C., Goff, S., Gilboa, E., Paskind, M., Mitra, S. W. & Baltimore, D. (1980) *Proc. Natl. Acad. Sci. USA* **77,** 3932–3936.
17. Gilboa, E., Goff, S., Shields, A., Yoshimura, F., Mitra, S. & Baltimore, D. (1979) *Cell* **16,** 863–874.
18. Benz, W. E., Jr., Wydro, R. M., Nadal-Ginard, B. & Dina, D. (1980) *Nature (London)* **288,** 665–669.
19. Shinnick, T. M., Lerner, R. A. & Sutcliffe, J. G. (1981) *Nature (London)* **293,** 543–548.
20. Payne, G. S., Courtneidge, S. A., Crittenden, L. B., Fadly, A. M., Bishop, J. M. & Varmus, H. E. (1981) *Cell* **23,** 311–322.
21. van der Putten, H., Quint, W., Raaij, J. V., Maandag, E. R., Verma, I. M. & Berns, A. (1981) *Cell* **24,** 729–739.
22. Tsichlis, P. N., Strauss, P. G. & Hu, L. F. (1983) *Nature (London)* **302,** 445–449.
23. Lemons, R. S., Nash, W. G., O'Brien, S. J., Benveniste, R. E. & Sherr, C. J. (1978) *Cell* **14,** 995–1005.